Pergamon

Tetrahedron: *Asymmetry* 13 (2002) 2593–2603

TETRAHEDRON: *ASYMMETRY*

A comparative study on the 1,3-dipolar cycloadditions of diazomethane and bis(diisopropylamino)phosphinodiazomethane to chiral electron-deficient olefins: reactivity and diastereoselectivity

Ona Illa,[a] Elena Muray,[a] Déborah Amsallem,[b] Albertina G. Moglioni,[a] Heinz Gornitzka,[b] Vicenç Branchadell,[a,*] Antoine Baceiredo[b,*] and Rosa M. Ortuño[a,*]

[a]*Departament de Química, Universitat Autònoma de Barcelona, 08193 Bellaterra, Barcelona, Spain*
[b]*Laboratoire Hétérochimie Fondamentale et Appliquée, Université Paul Sabatier, 118, route de Narbonne, F-31062 Toulouse Cedex 04, France*

Received 9 October 2002; accepted 29 October 2002

Abstract—The 1,3-dipolar cycloadditions of bis(diisopropylamino)phosphinodiazomethane, **10**, to chiral electron-deficient olefins have been investigated for the first time. The results have been compared with those corresponding to the reactions of diazomethane and the same or similar substrates. The experimental observations have been rationalized by DFT theoretical calculations. Diazomethane has been shown to be more reactive than **10** in all cases. The dipolarophiles include compounds synthesized from D-glyceraldehyde acetonide and (−)-verbenone. The latter compounds, bearing a *gem*-dimethylcyclobutane moiety, are less reactive than those derived from D-glyceraldehyde bearing a dioxolane ring. The influence of the *Z*/*E* geometry of the double bond on the reactivity and the π-facial diastereoselectivity has been investigated. Thus, in the reactions of diazomethane, the diastereoselectivity is not dependent on the *Z*/*E* stereochemistry but the reactivity is lower for (*E*)-cyclobutyl derivatives than for their *Z* isomers. In the reactions between **10** and the glyceraldehyde derivatives, the *E* isomers are less reactive than the *Z* ones and afford adducts with poor facial diastereoselectivity due to unfavorable interactions between the reactants in the corresponding transition states.

1. Introduction

Cyclopropane and pyrazoline moieties are present as structural units in the skeletons of many natural and designed products. Among the cyclopropane derivatives, amino acids,[1] peptidomimetics,[2] and nucleosides[3] are prominent and several synthetic methods have been developed for their preparation. Certain Δ^2-pyrazolines have displayed significant biological activities.[4] Much effort has been directed, therefore, to achieve efficient synthetic approaches to these compounds. The 1,3-dipolar cycloadditions of diazoalkanes to electron-deficient olefins offer synthetic entries to both types of molecules. Usually, diazoalkanes add to trisubstituted olefins to afford Δ^1-pyrazolines that can be photolyzed to the corresponding cyclopropanes, whereas Δ^1-pyrazolines resulting from the addition to disubstituted olefins can isomerize to Δ^2-tautomers that are not suitable for photolysis. Since the stereochemistry is conserved during the photochemical decomposition of Δ^1-pyrazolines,[5] good stereocontrol in the cycloaddition step is crucial to the diastereoselectivity of the whole cyclopropanation process of chiral olefins.

Empirical or theoretical models suggested to explain the π-facial diastereoselection of cycloaddition reactions, such as the *inside alkoxy* theory[6] or the principle of 1,3-allylic strain,[7] do not explain satisfactorily the stereochemical outcome of the reactions between diazomethane and chiral substrates as previously reported.[8] Recently, we studied the cycloadditions of diazomethane to chiral olefins **1**, **2**, **4**–**6** (Chart 1), prepared from D-glyceraldehyde acetonide, in order to establish the origin of the π-facial diastereoselection.[5,9]

All these molecules bear an alkoxy substituent, provided by the bulky dioxolane ring. *syn*-Adducts were obtained as the major isomers in all cases, independently of the *Z*/*E* stereochemistry of the double bond and the number and nature of the substituents. Theo-

* Corresponding authors. E-mail: vicenc@klingon.uab.es; baceired@chimie.ups-tlse.fr; rosa.ortuno@uab.es

0957-4166/02/$ - see front matter
PII: S0957-4166(02)00714-0

retical calculations performed on **4** and **6**, chosen as representative systems, showed that steric hindrance due to the bulky dioxolane group is the main factor governing the preference for the *syn*-attack of diazomethane to the olefinic double bond. Therefore, the origin of the π-facial diastereoselection in these cycloadditions is found in the chirality of the dioxolane stereogenic center, as the predominant feature determining the stereochemistry of the resulting adducts.

We also described the cycloaddition of diazomethane to cyclobutyl dehydroamino acid derivatives (*Z*)-**8** and (*Z*)-**9** (Chart 1), prepared from (–)-α-pinene, to afford adducts as single diastereoisomers.[10] The configuration of the new stereogenic centers could be explained by considering that, for the most stable conformers, the π-facial diastereoselection was the result of steric hindrance by the *gem*-dimethyl substituents and the side chain of the cyclobutane-ring.

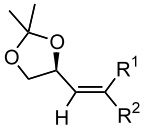

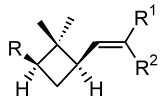

***Z*-1**, $R^1 = CO_2Me$, $R^2 = H$
***E*-1**, $R^1 = H$, $R^2 = CO_2Me$
***Z*-2**, $R^1 = SO_2Ph$, $R^2 = H$
***E*-2**, $R^1 = H$, $R^2 = SO_2Ph$
***E*-3**, $R^1 = H$, $R^2 = NO_2$
***Z*-4**, $R^1 = NO_2$, $R^2 = Me$
***E*-4**, $R^1 = Me$, $R^2 = NO_2$
***Z*-5**, $R^1 = CO_2Et$, $R^2 = Me$
***E*-5**, $R^1 = Me$, $R^2 = CO_2Et$
***Z*-6**, $R^1 = NHCbz$, $R^2 = CO_2Me$
***E*-6**, $R^1 = CO_2Me$, $R^2 = NHCbz$

***Z*-7**, $R^1 = H$, $R^2 = CO_2Me$
***E*-7**, $R^1 = CO_2Me$, $R^2 = H$
***Z*-8**, $R^1 = CO_2Me$, $R^2 = NHCbz$

R =

***Z*-9**, $R^1 = CO_2Me$, $R^2 = NHCbz$,
$R = CH_2CH_2OBn$

$(^iPr_2N)_2P-C(H)=N_2$ **10**

Chart 1.

Only one cycloaddition reaction involving bis(diisopropylamino)phosphinodiazomethane **10**[11] has been reported. Indeed, it reacted at 40°C with a monosubstituted achiral olefin with spontaneous loss of nitrogen to afford the corresponding cyclopropane derivative in near-quantitative yield. The high stereoselectivity of this cycloaddition is noteworthy, since the phosphino group and the substituent furnished by the olefin were in a *trans*-disposition.[12] The synthetic potential of this reagent is enormous since it can provide an entry to densely functionalized cyclic compounds.

Herein, we describe the first examples of the reaction between the phosphinodiazoalkane **10** and chiral substrates. The stereoselectivity of the cycloadditions regarding the π-facial diastereoselection and the *cis*/*trans* stereochemistry concerning the phosphino substituent has been investigated. The influence of the *Z*/*E* configuration of the olefin has also been considered. The experimental results have been rationalized by DFT theoretical calculations considering not only the conformational bias of the substrates but also the transition states leading to the diastereoisomeric adducts. From these results, the reactivity of **10** is compared with that of diazomethane towards the same dipolarophiles. The discrepancies in the stereoselectivity involved in the cycloadditions of both dipoles are also pointed out.

2. Results and discussion

2.1. Cycloaddition reactions and stereochemical assignments

The cycloadditions of **10**[11] to **1**, **2**, **3**, **5** and **7** were investigated and the cycloaddition of diazomethane to **7**, both *Z* and *E* isomers, was also studied. Olefins **1**,[13] **2**,[14] **5**,[15] as pure *Z* and *E* diastereoisomers, as well as (*E*)-**3**[16] were synthesized according to the procedures described in the literature. D-Glyceraldehyde was the chiral precursor bearing the stereogenic centre (*S* configuration) that must induce π-facial diastereoselection in the addition of the dipoles to these substrates. In turn, (*Z*)- and (*E*)-**7** were synthesized from (–)-verbenone which provides the (1*R*,3*R*) configuration for the stereogenic centers of the cyclobutane-ring.[17] The methods used involve Wittig or Wittig–Horner condensations, except for (*E*)-**3**, which was synthesized through nitroaldol reaction between D-glyceraldehyde and nitromethane.

Previously, we have shown that excess diazomethane reacts with substrates **1**, **2**, **4**–**6**, as pure *Z* or *E* isomers, under the conditions shown in Table 1 to afford the corresponding adducts in high yields (entries 1, 3, 5, 7–13). *syn*-Adducts were always the major products obtained in 82–100% de (Fig. 1).[5,9] Nitro olefin (*E*)-**3**

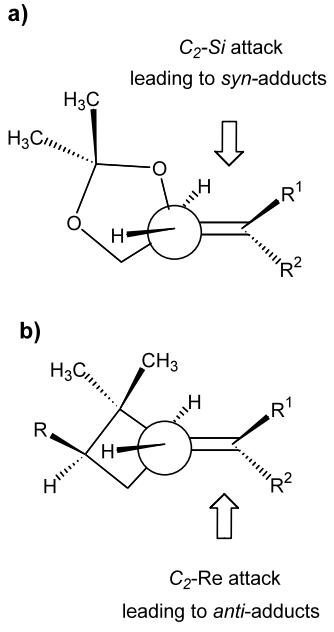

Figure 1. Newman projections for the conformers considered to define *syn*/*anti* adducts: (a) for substrates **1**–**6**; (b) for substrates **7**–**9**.

Table 1. Reaction conditions, stereochemistry of the major adduct, yield, and *syn*/*anti* diastereomeric excess (% d.e.) in the additions of diazomethane (CH_2N_2) and phosphinodiazocompound **10** to olefins **1**–**9**[a]

Entry	Olefin	Dipole	*T* (°C)	Time (h)	Adduct[b]	% Yield[c]	% d.e.	Ref.
1	(*Z*)-**1**	CH_2N_2	rt	2.5	*syn*	90	96	9
2	(*Z*)-**1**	**10**	60	2	*syn*	75[d]	94[f]	This work
3	(*E*)-**1**	CH_2N_2	rt	2.5	*syn*	90	96	9
4	(*E*)-**1**	**10**	70	20	*anti*	28[d]	5[f]	This work
5	(*Z*)-**2**	CH_2N_2	0	1.5	*syn*	70	>98	9
6	(*Z*)-**2**	**10**	6	20	*syn*	25[d]	100[f]	This work
7	(*E*)-**2**	CH_2N_2	0	1.5	*syn*	75	>98	9
8	(*Z*)-**4**	CH_2N_2	0	1	*syn*	75	84	9
9	(*E*)-**4**	CH_2N_2	0	1	*syn*	76	82	9
10	(*Z*)-**5**	CH_2N_2	rt	3	*syn*	90	86	9
11	(*E*)-**5**	CH_2N_2	rt	3	*syn*	71	84	9
12	(*Z*)-**6**	CH_2N_2	rt	3	*syn*	100	>98	5, 9
13	(*E*)-**6**	CH_2N_2	rt	3	*syn*	100	>98	5, 9
14	(*Z*)-**7**	CH_2N_2	rt	20	*anti*	50[e]	>98[g]	This work
15	(*E*)-**7**	CH_2N_2	rt	20	*anti*	95	>98[g]	This work
16	(*Z*)-**8**	CH_2N_2	rt	20	*anti*	80	>98	10
17	(*Z*)-**9**	CH_2N_2	rt	20	*anti*	83	>98	10

[a] Olefins (*E*)-**2**, (*E*)-**3**, (*Z*)-**5**, (*E*)-**5**, (*Z*)-**7**, and (*E*)-**7** (see Chart 1) did not react with **10** under several conditions tried.
[b] Referred to the major isomer.
[c] Isolated yield referred to the major isomer.
[d] Isolated yield after thiolation referred to the major isomer.
[e] Conversion ratio.
[f] Determined by ^{31}P NMR spectroscopy.
[g] Determined by ^{1}H NMR spectroscopy.

afforded adducts contaminated with much undefined and polymeric material.

Otherwise, *anti*-adducts (Fig. 1) were the only diastereomers produced from the reactions between diazomethane and olefins (*Z*)-**8** and (*Z*)-**9** (Table 1, entries 16, 17).[10]

In this work, diazocompound **10** was allowed to react with (*Z*)-**1** in a THF solution at 60°C for 2 h to afford a 97:3 mixture of Δ^2-pyrazolines *syn*- and *anti*-**11** (Scheme 1). The progress of the reaction was easily monitored by ^{31}P NMR spectroscopy following the disappearance of the peak at 48.00 ppm concomitant to the appearance of two peaks at 44.90 and 45.98 ppm corresponding to both isomers. The reaction did not take place at room temperature. The results were similar when one or 3 equiv. of **10** were used. The adducts **11** were treated in situ with an excess of elemental sulphur to produce the corresponding thioxo derivatives *syn*- and *anti*-**12** in 75% yield after purification. The major product was isolated by column chromatography and fully characterized as a pale yellow solid. An X-ray diffraction analysis allowed the unequivocal assignment of configuration to the two new stereogenic centers and the identification of this compound as *syn*-**12** (Fig. 2)[18] (^{31}P NMR: δ 76.0, $[\alpha]_D$ +313.7). The minor isomer was identified as described below. The relative stereochemistry of the phosphino and dioxolanyl groups was *trans* in both diastereoisomers.

Several conditions were tried for the cycloaddition of **10** to olefin (*E*)-**1** which was shown to be much less reactive than (*Z*)-**1**. Under the optimal conditions

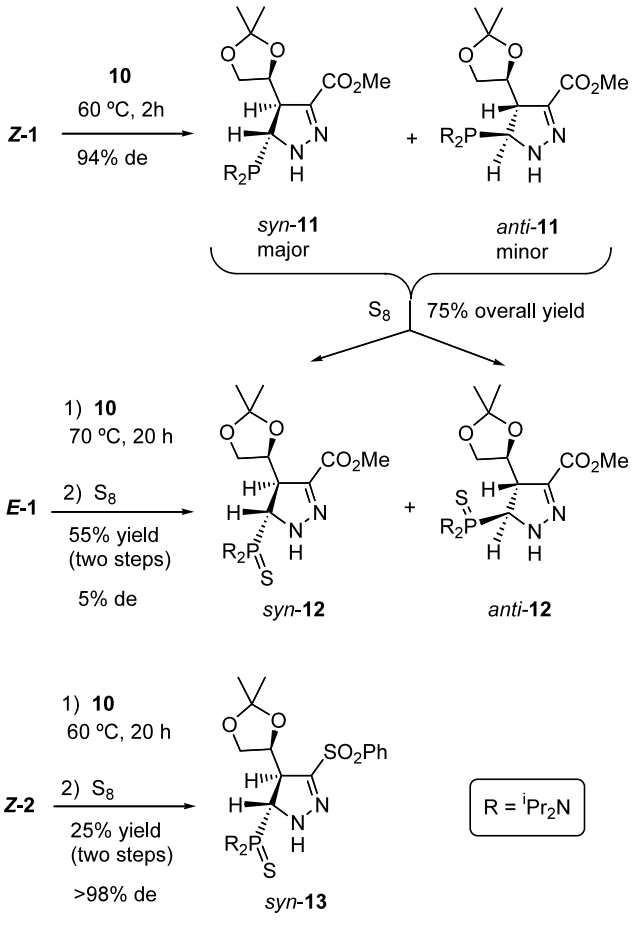

Scheme 1.

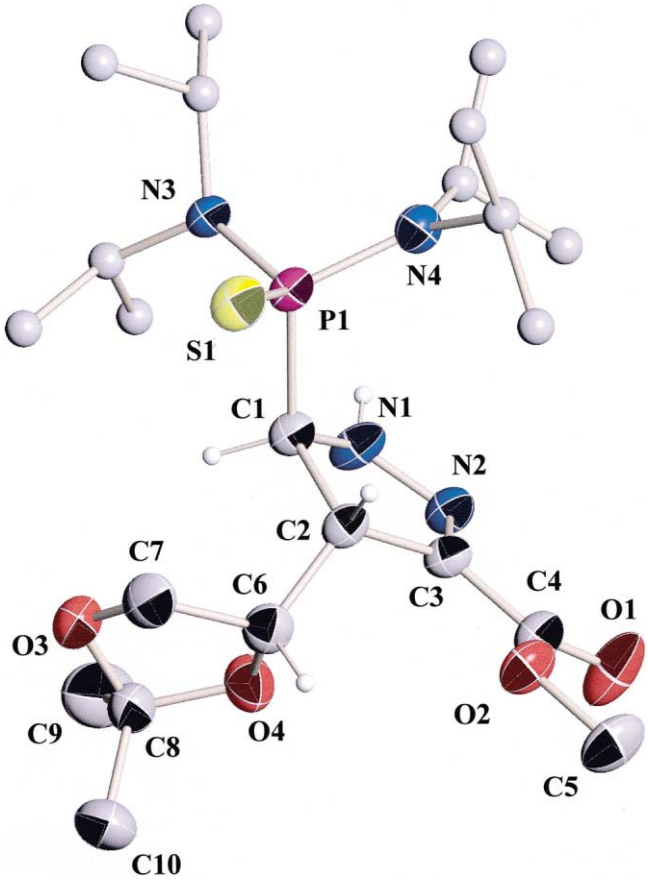

Figure 2. Thermal ellipsoid diagram (50% probability) of *syn*-**12** showing the atom numbering scheme. Only one molecule of the asymmetric unit is presented. Isopropyl groups have been simplified and most of the H atoms have been omitted for clarity.

found, (*E*)-**1** reacted with 3 equiv. of **10** in THF at 70°C for 20 h to produce a ca. 1:1 mixture of diastereoisomeric adducts *syn*- and *anti*-**11** which, after thiolation and subsequent purification, afforded *syn*- and *anti*-**12** in 55% yield and only 5% de. The later product (^{31}P NMR: δ 72.3, $[\alpha]_D$ −419.0) was the major isomer and it could be isolated by column chromatography and submitted to an X-ray diffraction analysis to secure its unambiguous identification (Fig. 3).[18] Thus, π-facial diastereoselection, responsible for *syn*/*anti* stereochemistry, is almost null in this reaction. Nevertheless, the stereoselectivity (wrt the relative disposition of the phosphino and the dioxolanyl groups) was excellent, providing a *trans*-relationship of these substituents in both adducts.

Vinyl sulphones **2** were less reactive than unsaturated esters **1** in the cycloadditions to **10**, the dependence of the reactivity on the *Z*/*E* stereochemistry being more evident indeed. Thus, (*Z*)-**2** reacted with **10** in THF at 60°C for 20 h to afford, after treatment with elemental sulphur, only one pyrazoline in 25% yield. This compound was identified as *syn*-**13** on the basis of NOESY correlations (Fig. 4) and NOE-1D experiments that allowed us to assign not only the configuration of the

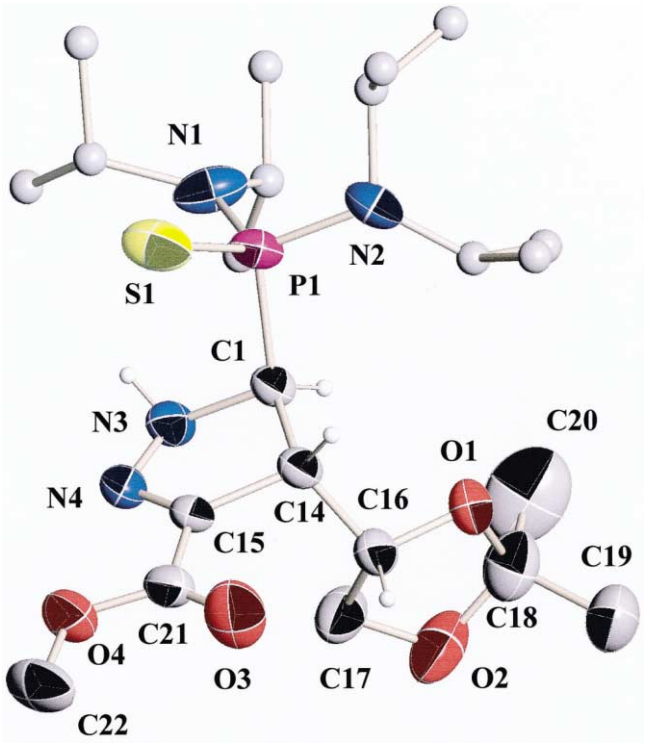

Figure 3. Thermal ellipsoid diagram (50% probability) of *anti*-**12** showing the atom numbering scheme. Isopropyl groups have been simplified and most of the H atoms have been omitted for clarity.

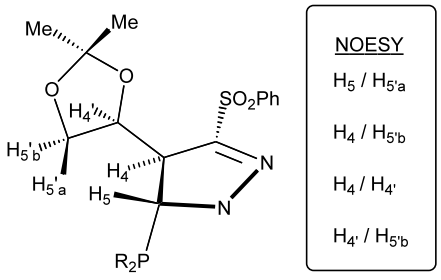

Figure 4. Stereochemical assignment of *syn*-**13** on the basis of NOESY correlations.

newly created stereogenic centers but also the preferential conformation for the dioxolane ring.

Attempts to react **10** with (*E*)-**2** and (*E*)-**3** under several conditions failed. Moreover, diazoalkane **10** decomposed when exposed at high temperatures for long reaction times.

Otherwise, phosphinodiazo compound **10** did not react with trisubstituted olefins like **5** in contrast with the results from the reactions between diazomethane and **4**, **5** or **6** (both *Z*/*E* isomers) that afforded adducts in good yields (Table 1, entries 8–13).[9]

Reactions with substrates (*Z*)- and (*E*)-**7** were also considered to investigate the steric hindrance by the bulky *gem*-dimethylcyclobutyl moiety in disubstituted

olefins. After treatment of (*Z*)- or (*E*)-**7** with **10** (3 equiv.) at 50°C for 6 days, only traces of adducts were detected (^{31}P NMR: δ 75.0 from (*Z*)-**7** and 74.9 from (*E*)-**7**), along with many decomposition substances. In contrast, (*Z*)-**7** was made to react with excess of diazomethane at room temperature overnight to afford Δ^1-pyrazoline **15** along with ca 50% recovered starting material (Scheme 2). Significant further conversion was not observed after longer periods of time but Δ^2-pyrazoline **17** was then produced. This compound also resulted when isolation of **15** was attempted by chromatography of the reaction mixture.

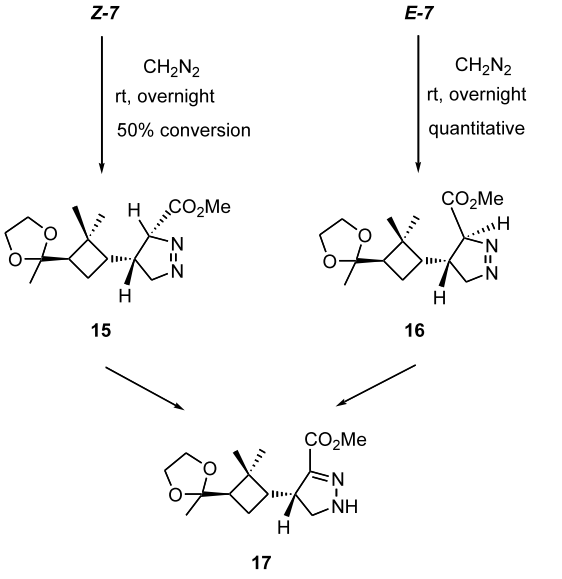

Scheme 2.

Olefin (*E*)-**7** was more reactive and afforded quantitatively **16** after treatment with an excess of diazomethane under similar conditions as (*Z*)-**7**. Δ^1-pyrazoline **16** tautomerized slowly to Δ^2-pyrazoline **17** on standing at room temperature. Therefore, for these substrates, the reactivity towards diazomethane was strongly dependent on the *Z*/*E* geometry of the double bond but the stereoselectivity of the cycloaddition was the same in both cases since a single *anti* diastereomer was formed in every case. (Table 1, entries 14, 15). The stereochemistry of pyrazolines **15**–**17** was assigned to be *anti*, as depicted in Scheme 2, by comparison with the adducts resulting from the cycloaddition of diazomethane to olefins (*Z*)-**8** and (*Z*)-**9** whose configuration was unambiguously determined by X-ray analysis.[10]

It is noteworthy to remark that the substrates derived from verbenone, **7**–**9**, are less reactive than the family of substrates derived from D-glyceraldehyde acetonide, **1**–**6**. Thus, it seems that the high steric requirements of the *gem*-dimethyl substituted cyclobutane moiety in **7**–**9** impede the approach of the dipoles, accounting for the lower reactivity of these compounds.

2.2. Theoretical calculations

In order to rationalize the experimental results concerning the reactivity of these systems as well as the stereoselectivity of the cycloadditions considered, theoretical calculations were carried out for selected reactions. Fig. 5 presents the optimized structures of (*Z*)-**1**, (*E*)-**1**, (*Z*)-**18**, and (*E*)-**18**, where **18** is a model of **7** in which the 2-methyl-1,3-dioxolanyl group has been replaced, for simplicity, by an acetyl group (Chart 2).

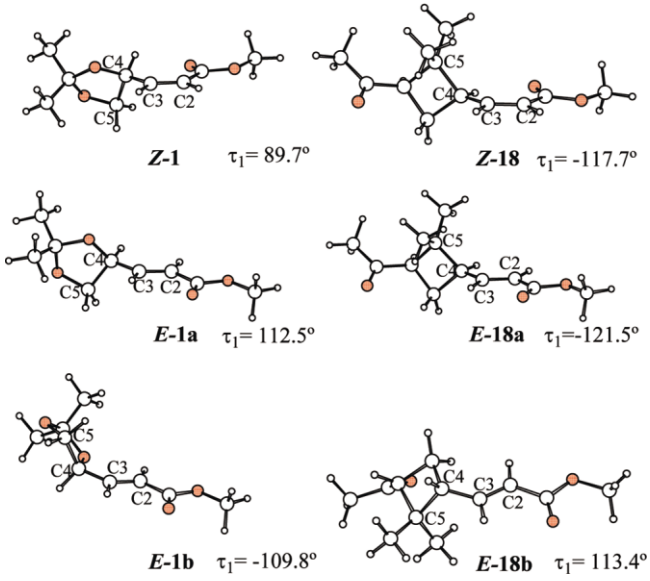

Figure 5. Optimized structures of olefins **1** and **18**. τ_1 is the C2–C3–C4–C5 dihedral angle.

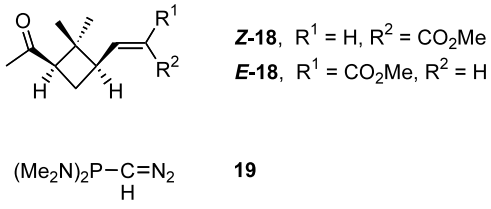

Chart 2.

In all cases, we have considered all possible structures arising from the rotation around C3–C4. For the *Z* isomers there is only one conformational minimum. The rotational barriers are 7.4 kcal mol^{-1} for (*Z*)-**1** and 7.5 kcal mol^{-1} for (*Z*)-**18**. On the other hand, for the *E* isomers there are two different conformers, that we have denoted as **a** and **b**. (*E*)-**1b** is more stable than (*E*)-**1a** ($\Delta G = 0.2$ kcal mol^{-1}), whereas for (*E*)-**18** the most stable conformer is (*E*)-**18a** ($\Delta G = 0.5$ kcal mol^{-1}). The rotational barriers are 3.2 kcal mol^{-1} for (*E*)-**1** and 2.5 kcal mol^{-1} for (*E*)-**18**.

We have studied the attack of diazomethane to both geometrical isomers of **1** and **18**. For each system we have considered the attack of the dipole to both π-faces of the olefin. Figs. 6 and 7 present the structures of the transition states corresponding to these reactions. For (*E*)-**1** and (*E*)-**18** we have considered the attack to both

Table 2. Activation Gibbs energies, at 1 atm and 298.15 K, and selected geometry parameters corresponding to the transition states of the reactions of olefins **1** and **18** with diazomethane and **19**

Olefin	Dipole	TS[a]	$\Delta G^{\ddagger}$[b]	C1–C3[c]	N1–C2[c]	τ_1[d]	τ_2[e]	τ_3[f]
(*Z*)-**1**	CH_2N_2	*syn*	25.6	2.20	2.59	77.0 (−12.7)	2.2	
		anti	29.3	2.20	2.62	70.6 (−19.1)	−8.5	
(*E*)-**1**	CH_2N_2	*syn*	24.6	2.20	2.60	85.6 (−26.9)	4.5	
		anti	27.3	2.22	2.55	−63.9 (+45.9)	−3.7	
(*Z*)-**18**	CH_2N_2	*syn*	30.7	2.23	2.54	175.3 (−67.0)	0.0	
		anti	28.8	2.20	2.55	−82.2 (+35.5)	1.7	
(*E*)-**18**	CH_2N_2	*syn*	28.9	2.23	2.54	−179.3 (−36.2)	10.0	
		anti	27.7	2.20	2.55	−83.1 (+38.4)	−7.6	
(*Z*)-**1**	**19**	*syn*	31.4	2.17	2.45	77.7 (−12.0)	13.2	−15.0 (−56.7)
		anti	35.1	2.17	2.47	71.1 (−18.6)	−15.0	10.2 (+51.9)
(*E*)-**1**	**19**	*syn*	33.2	2.16	2.49	84.4 (−28.1)	2.6	−46.5 (−88.2)
		anti	34.3	2.20	2.46	−66.3 (+43.5)	1.2	33.8 (+75.5)

[a] See Figs. 6, 7 and 8.
[b] In kcal mol^{-1}.
[c] In Å.
[d] C2–C3–C4–C5 dihedral angle in degrees. In parentheses variation with respect to the isolated olefin.
[e] C2–C3–C1–N2 dihedral angle in degrees.
[f] N2–C1–P–N3 dihedral angle in degrees. In parentheses variation with respect to isolated **19**.

conformers and the structures presented in Figs. 6 and 7 correspond to the most favorable ones. Activation Gibbs energies and selected geometry parameters corresponding to the transition states are shown in Table 2.

We have also studied the attack of bis(dimethylamino)phosphinodiazomethane **19**, as a model of **10**, to **1** (Chart 2). For this process, in addition to the π-facial selectivity (*syn*/*anti*) two different stereoisomers related to the *cis* or *trans* arrangement of the phosphino group and the olefin substituent a C3 can be formed. Preliminary calculations using phosphinodiazomethane as a model have shown that the *trans* transition states are always more favorable than the *cis* ones. For this reason, only *trans* transition states have been considered for the attack of **19** to **1**. Fig. 8 shows the structures of these transition states and the corresponding activation Gibbs energies and selected geometry parameters have been included in Table 2. We can

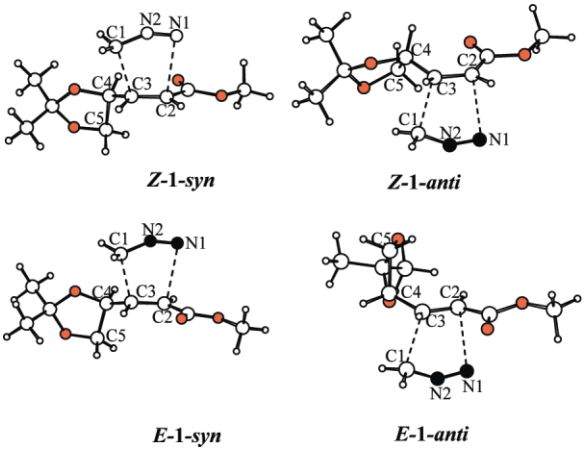

Figure 6. Structures of the transition states corresponding to the reaction of diazomethane with **1**.

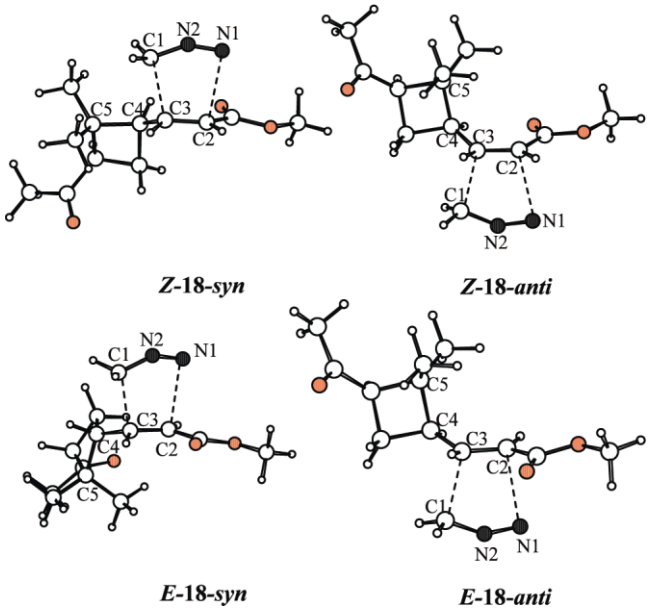

Figure 7. Structures of the transition states corresponding to the reaction of diazomethane with **18**.

observe that the interatomic distances corresponding to the two forming bonds do not significantly change from one transition state to another, C1–C3 distances ranging between 2.16 and 2.23 Å and N1–C2 distances ranging between 2.46 and 2.62 Å.

For the reactions of diazomethane with (*Z*)- and (*E*)-**1** the *syn* attack is kinetically more favorable than the formation of the *anti* products, in excellent agreement with the experimentally observed diastereoselectivity. Moreover, (*E*)-**1** is predicted to be slightly more reactive than (*Z*)-**1**. According to Table 2, olefins (*Z*)- and (*E*)-**18** are less reactive towards diazomethane than (*Z*)- and (*E*)-**1**, in good accordance with the experimental results. Regarding the diastereoselectivity, *anti* transi-

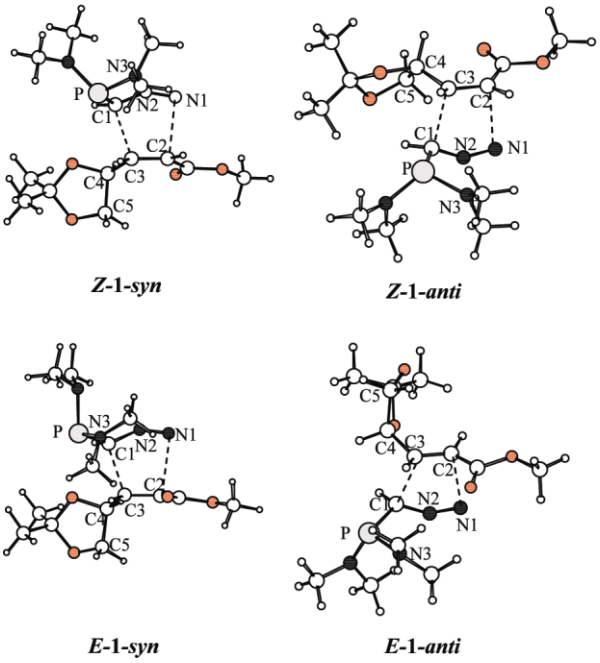

Figure 8. Structures of the transition states corresponding to the reaction of **19** with **1**.

tion states are predicted to be the most favorable ones, as it has been observed for the reactions of (*Z*)- and (*E*)-**7**. The differences between *syn* and *anti* activation Gibbs energies (1.9–1.2 kcal mol^{-1}) are lower than those corresponding to the reactions of (*Z*)- and (*E*)-**1** (2.7–3.7 kcal mol^{-1}), so that reactions of (*Z*)- and (*E*)-**18** with diazomethane are predicted to be less selective than reactions of (*Z*)- and (*E*)-**1**. This result is not in agreement with the observed diastereoselectivities for (*Z*)- and (*E*)-**7**.

For the attack of **19** to (*Z*)- and (*E*)-**1** the Gibbs activation energies are notably higher than the values corresponding to the attack of diazomethane, so that the reaction is expected to be much slower, in excellent agreement with the experimental results corresponding to the reactions of **10**. Regarding the selectivity, there is a remarkable difference between both geometrical isomers: for (*Z*)-**1** the difference between *anti* and *syn* activation Gibbs energies is 3.7 kcal mol^{-1}, whereas for (*E*)-**1** the difference is only 1.1 kcal mol^{-1}. If we compare these values with those corresponding to the reaction with diazomethane, we can observe that for the *syn* transition states the relative reactivity of (*Z*)- and (*E*)-**1** towards diazomethane and **19** are different. For diazomethane the most reactive isomer is (*E*)-**1**, whereas for **19** (*Z*)-**1** is more reactive than (*E*)-**1**. On the other hand, for the *anti* transition states both diazomethane and **19** show the same trend. This result suggests that the low selectivity observed for the reaction between **19** and (*E*)-**1** is due to a destabilization of the *syn* transition state.

There are two ways to relieve steric repulsion between the olefin and the incoming dipole molecule: a rotation around the C3–C4 bond (τ_1) and a rotation around the C1–C3 axis (τ_2) (see Fig. 9). When the dipole is **19** the variation of the N2–C1–P–N3 dihedral angle (τ_3) is also involved in the lowering of steric repulsion.

For the reaction of diazomethane with (*Z*)-**1** the formation of the *syn* product involves the attack to the less hindered face of the olefin. On the other hand, the formation of the *anti* product involves the attack of diazomethane to the more hindered face and so a larger geometry distortion is required, as it can be observed from the variation of τ_1 and τ_2 (Table 2). The (*E*)-**1**-*syn* transition state comes from the attack of diazomethane to the (*E*)-**1a** conformer and the (*E*)-**1**-*anti* transition state corresponds to the attack to the (*E*)-**1b** conformer. Rotation around C3–C4 is easier for (*E*)-**1**, so that relief of steric repulsion with the incoming diazomethane molecule is more efficient than for (*Z*)-**1**. As a consequence, potential energy barriers corresponding to the reaction of diazomethane with (*E*)-**1** are lower than those corresponding to (*Z*)-**1**.

For the reactions of (*E*)-**18** with diazomethane, we can observe that the *syn* transition state comes from the attack of diazomethane to the (*E*)-**18b** conformer and that the *anti* transition state corresponds to the attack of diazomethane to (*E*)-**18a**. If we compare the variation of τ_1 when going from the reactant to the transition state for (*E*)-**1**-*syn* and (*E*)-**18**-*anti* transition states (see Table 2), we can observe a larger distortion in the latter case. This fact seems to indicate that the difference in reactivities between (*E*)-**1** and (*E*)-**18** is due to steric effects related to the *gem*-dimethyl group. A similar conclusion can be reached from the comparison between (*Z*)-**1**-*syn* and (*Z*)-**18**-*anti* transition states.

For the reactions of **19** with (*Z*)-**1** and (*E*)-**1**, the variation of the C2–C3–C4–C5 dihedral angle (τ_1) when going from isolated olefin to the transition states is similar to that observed for the attack of diazomethane. For the transition states corresponding to the reaction of (*Z*)-**1** torsion around C1–C3 (τ_2) is larger than for the reactions of diazomethane, whereas for the transitions states corresponding to the reactions of (*E*)-**1** the deviation from planarity is insignificant. This torsion is hindered by the steric repulsion between the bis-(dimethylamino)groups of **19** and the ester group of (*E*)-**1**.

For the optimized equilibrium geometry of **19** the N3–P–C1–N2 dihedral angle (τ_3) is 41.7° (when it is

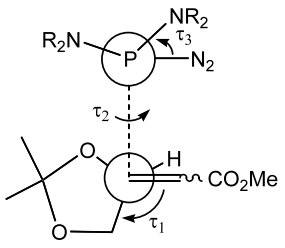

Figure 9. Newman projection corresponding to the approximation of dipole **19** to olefin **1**.

oriented as in the *syn* transition states). So, the P lone pair is perpendicular to the C1–N2–N1 axis (see Fig. 9). When **19** attacks the olefin, a significant rotation around C1–P is produced in order to minimize repulsion. For (*Z*)-**1**-*syn* and (*E*)-**1**-*syn* transition states, the phosphorus atom and one of the dioxolane oxygens are close enough to induce repulsion (P–O distances are 3.75 and 3.68 Å, respectively) due to the orientation adopted by the dioxolane ring (Fig. 8). This repulsion can be relieved through rotation around C3–C1 or around C1–P. As we have already mentioned, for (*E*)-**1**-*syn* rotation around the C3–C1 axis is hindered by steric repulsion between the $N(Me)_2$ and ester groups, so that the variation of τ_3 is larger than for the (*Z*)-**1**-*syn* transitions state.

The rotation around C1–P (τ_3) in (*E*)-**1**-*syn* transition state moves one of the $N(Me)_2$ groups of **19** towards the ester group or the (*E*)-**1**, thus generating steric repulsion. This kind of interaction is absent in (*Z*)-**1**-*syn* (Fig. 8).

So, the lower stereoselectivity of (*E*)-**1** relative to (*Z*)-**1** in their reactions with **19** can be attributed to the destabilization of the (*E*)-**1**-*syn* transition state due to a repulsion between P and dioxolane oxygen lone pairs and to steric hindrance between the $N(Me)_2$ and ester groups. This effect is expected to be more important when the dipole is **10**, since the *i*-Pr groups are much more cumbersome than the methyl groups used in calculations.

3. Concluding remarks

From these studies, we can conclude that diazomethane is much more reactive than the phosphinodiazoalkane **10** towards all of the dipolarophiles considered.

In turn, the family of substrates derived from D-glyceraldehyde acetonide is more reactive towards both dipoles than the olefins synthesized from (–)-verbenone. The higher steric congestion produced by the bulky 3′-substituted *gem*-dimethylcyclobutane moiety can account for the lower reactivity of **7**–**9**.

For the two families of dipolarophiles, theoretical calculations predict *E* isomers to be more reactive than their *Z* counterparts due to the lower restrictions in the rotation around the bond linking one of the olefinic carbons and the bulkiest substituent (dioxolane or cyclobutane). In the reactions with diazomethane, this dependence on the *Z*/*E* geometry is experimentally observed only for the cyclobutyl derivatives (*Z*)- and (*E*)-**7**. These compounds do not react with the phosphinodiazoalkane **10**.

In contrast, (*E*)-**1** and (*E*)-**2** react with **10** much more slowly than (*Z*)-**1** and (*Z*)-**2**, in good accordance with the theoretical calculations, due to repulsive interactions between the dipole and both substituents of the C–C double bond in the substrates. These unfavorable interactions are also responsible for the low π-facial diastereoselectivity observed in the cycloaddition of (*E*)-**1** to **10**.

4. Experimental

4.1. General

All manipulations involving diazo compound **10** were performed under a nitrogen atmosphere using standard Schlenk techniques and dry, oxygen-free solvents were employed. Flash column chromatography was carried out on silica gel (240–400 mesh). Melting points were determined on a hot stage and are uncorrected. Signals in IR spectra are reported in cm^{-1}. In the 250 or 500 MHz ^1H, 62.5 MHz ^{13}C, and 101.2 MHz ^{31}P NMR spectra, chemical shifts are given on the δ scale. Coupling constants (*J*) are given in Hz. Electron impact mass spectra were recorded at 70 eV.

4.2. Computational details

All calculations have been done using density functional (DFT) methods within the generalized gradient approximation (GGA). Molecular geometries have been fully optimized using Becke's[19] functional for exchange and the correlation functional due to Perdew and Wang[20] (BPW91). The level of calculation has been shown to provide excellent results for the reaction between diazomethane and ethylene.[21] Molecular geometries have been fully optimized at this level of calculation using the standard 6-31G(d) basis set.[22] Harmonic vibrational frequencies have been calculated for all structures to characterize them as energy minima (all frequencies are real) or transition states (one and only one imaginary frequency). These calculations have been done with the Gaussian-98 program.[23] In order to minimize the basis set superposition error, single point calculation have been done for the previously optimized geometries using an uncontracted Slater type orbital (STO) triple-ζ basis set supplemented with a set of *d* polarization functions for C, N, and O, and with a set of *p* functions for H (TZP). These calculations have been done using the ADF program.[24] The reported Gibbs energies at 1 atm and 298.15 K have been calculated from energies computed with the TZP basis set, whereas zero-point and thermal corrections to the energy and entropies have been calculated from frequencies computed with the 6-31G(d) basis set.

4.3. Crystallographic details

All data were collected at low temperature using an oil-coated shock-cooled crystal on a Bruker-AXS CCD 1000 diffractometer. Both structures were solved by direct methods (SHELXS-97)[25] and refined using the least-squares method on F^2.[26] Crystallographic data (excluding structure factors) have been deposited with the Cambridge Crystallographic Data Centre as supplementary publication No CCDC 194968 (for *syn*-**12**) and 194969 (for *anti*-**12**). Copies of the data can be obtained free of charge on application to CCDC, 12

Union Road, Cambridge CB21EZ, UK (fax: (+44) 1223-336-033; e-mail: deposit@ccdc.cam.ac.uk).

Crystal data for *syn*-12: $C_{24.5}H_{49}N_4O_4PS$, M = 526.71, monoclinic, *C*2, $a = 24.6842(16)$, $b = 10.1743(6)$, $c = 24.8571(16)$ Å, $\beta = 108.117(1)°$, $V = 5933.2(6)$ Å^3, $Z = 8$, $\rho_c = 1.179$ Mg m^{-3}, $F(000) = 2296$, $\lambda = 0.71073$ Å, $T = 193(2)$ K, μ(Mo Kα) = 0.197 mm^{-1}, crystal size 0.1×0.2×0.6 mm, $1.72° \leq \Theta \leq 24.71°$, 22729 reflections (10074 independent, $R_{int} = 0.0297$) and 711 parameters were refined. Largest electron density residue: 0.634 e Å^{-3}, R_1 (for $I > 2\sigma(I)$) = 0.0390 and $wR_2 = 0.0986$ (all data).

Crystal data for *anti*-12: $C_{22}H_{43}N_4O_4PS$, M = 490.63, monoclinic, $P2_1$, $a = 8.8265(4)$, $b = 17.2015(8)$, $c = 9.9600(5)$ Å, $\beta = 115.605(1)°$, $V = 1363.71(11)$ Å^3, $Z = 2$, $\rho_c = 1.195$ Mg m^{-3}, $F(000) = 532$, $\lambda = 0.71073$ Å, $T = 193(2)$ K, μ(Mo Kα) = 0.210 mm^{-1}, crystal size 0.2×0.3×0.3 mm, $2.27° \leq \Theta \leq 25.35°$, 11252 reflections (4968 independent, $R_{int} = 0.0340$) and 428 parameters were refined. Largest electron density residue: 0.279 e Å^{-3}, R_1 (for $I > 2\sigma(I)$) = 0.0452 and $wR_2 = 0.1070$ (all data).

4.4. General procedure for the cycloadditions of phosphinodiazocompound 10 to substrates (*Z*)-1, (*E*)-1, and (*Z*)-2

Temperature and reaction time is shown in Table 1 for each reaction (entries 2, 4, 6). The procedure for the cycloaddition of **10** to olefin (*Z*)-**1** is described. A solution of (*Z*)-**1** (400 mg, 2.2 mmol) in THF (5 mL) was added to phosphinodiazocompound **10** (570 mg, 2.1 mmol) and the mixture was stirred at 60°C for 2 h. The progress of reaction was monitored by ^{31}P NMR spectroscopy. When the reaction was complete the solution mixture was evaporated under vacuum, and the phosphinopyrazolines **11** were analyzed without any further purification to determine the diastereomeric excess. Treatment of a THF solution of phosphinopyrazolines **11** with an excess of elemental sulphur (100 mg) gave the corresponding thioxo derivatives **12**, which were purified by column chromatography on silica gel (1:1 hexane–ether as eluent). Chemical yields for the major isomers and diastereomeric excesses are shown in Table 1. Spectroscopic and analytical data are listed below.

4.4.1. (4*R*,5*R*)-5-[Bis(diisopropylamino)thioxophosphoranyl]-4-[2′,2′-dimethyl-(4′*S*)-1′,3′-dioxolan-4′-yl]-3-methoxycarbonyl-1*H*-pyrazoline, *syn*-12. Mp 54–57°C (from pentane); $[\alpha]_D$ +313.7 (*c* 0.77, ether); IR (KBr): 1701; ^{31}P NMR ($CDCl_3$): 76.00; ^{1}H NMR ($CDCl_3$): 1.24–1.37 (complex absorption, 30H, NCHCH_3 and OCCH_3), 3.50–3.70 (complex absorption, 4H, NCHCH$_3$), 3.76 (s, 3H, OCH_3), 3.91 (dd, $^2J_{HH} = 8.7$, $^3J_{HH} = 6.4$, 1H, $H_{5'a}$), 4.07 (dt, $^3J_{PH} = 27.4$, $^3J_{HH} = 4.9$, 1H, H_4), 4.30 (dd, $^2J_{HH} = 8.7$, $^3J_{HH} = 6.7$, 1H, $H_{5'b}$), 4.39 (m, 2H, $H_{4'}$, H_5); ^{13}C NMR ($CDCl_3$): 23.20–26.45 (6C, NCHCH$_3$ and OCCH$_3$), 47.33–47.64 (4C, NCHCH$_3$), 51.46–51.99 (2C, C_4 and OCH$_3$), 66.58 (d, $^1J_{PC} = 83.9$, C_5), 67.07 ($C_{5'}$), 74.53 (d, $^3J_{PC} = 16.2$, $C_{4'}$), 108.54 ($C_{2'}$), 141.33 (C_3), 162.31 (C=O). Anal. calcd for $C_{22}H_{34}N_4O_4PS$: C, 53.86; H, 8.83; N, 11.42; S, 6.53. Found: C, 53.94; H, 8.93; N, 10.95; S, 6.04%.

4.4.2. (4*S*,5*S*)-5-[Bis(diisopropylamino)thioxophosphoranyl]-4-[2′,2′-dimethyl-(4′*S*)-1′,3′-dioxolan-4′-yl]-3-methoxycarbonyl-1*H*-pyrazoline, *anti*-12. Mp 112–114°C (from pentane); $[\alpha]_D$ −419.0 (*c* 0.84, ether); IR (KBr): 1703; ^{31}P NMR ($CDCl_3$): 72.35; ^{1}H NMR ($CDCl_3$): 1.30–1.38 (complex absorption, 30H, NCHCH_3 and OCCH_3), 3.70–3.95 (complex absorption, 6H, NCHCH$_3$, $H_{5'a}$, $H_{5'b}$), 3.81 (s, 3H, OCH_3), 4.07 (dt, $^3J_{PH} = 26.4$, $^3J_{HH} = 4.2$, 1H, H_4), 4.43 (dd, $^3J_{HH} = 4.2$, $^2J_{PH} = 1.5$, 1H, H_5), 4.63 (ddt, $^3J_{HH} = 6.8$, $^3J_{HH} = 4.2$, $^4J_{PH} = 0.9$, 1H, $H_{4'}$); 6.60 (d, $^3J_{PH} = 7.3$, 1H, NH), ^{13}C NMR ($CDCl_3$): 23.70–26.30 (6C, NCHCH$_3$ and OCCH$_3$), 47.63–47.93 (4C, NCHCH$_3$), 49.09–52.19 (2C, C_4 and OCH$_3$), 64.02 (d, $^1J_{PC} = 87.7$, C_5), 66.27 ($C_{5'}$), 75.11 (d, $^3J_{PC} = 16.2$, $C_{4'}$), 109.41 ($C_{2'}$), 143.19 (C_3), 162.45 (C=O). Anal. calcd for $C_{22}H_{34}N_4O_4PS$: C, 53.86; H, 8.83; N, 11.42; S, 6.53. Found: C, 53.82; H, 8.96; N, 10.93; S, 6.31%.

4.4.3. (4*R*,5*R*)-5-[Bis(diisopropylamino)thioxophosphoranyl]-4-[2′,2′-dimethyl-(4′*S*)-1′,3′-dioxolan-4′-yl]-3-phenylsulphonyl-1*H*-pyrazoline, *syn*-13. Mp 135–137°C (from pentane); $[\alpha]_D$ +210.38 (*c* 0.77, CH_2Cl_2); IR (film) 3374, 1551, 981; ^{31}P NMR ($CDCl_3$): 76.55; ^{1}H NMR ($CDCl_3$): 1.16–1.39 (complex absorption, 30H, NCHCH_3 and OCCH_3), 3.36–3.6 (complex absorption, 4H, NCHCH$_3$), 4.04 (dd, $^2J_{HH} = 9.1$, $^3J_{HH} = 6.6$, 1H, $H_{5'a}$), 4.35 (ddd, $^3J_{PH} = 27.7$, $^3J_{HH} = 5.6$, $^3J_{HH} = 3.7$, 1H, H_4), 4.42 (m, 2H, $H_{5'}$, H_5), 4.65 (ddd, $^3J_{HH} = 6.6$, $^3J_{HH} = 6.4$, $^3J_{HH} = 3.7$, 1H, $H_{4'}$), 6.30 (d, $^3J_{PH} = 5.5$, 1H, NH), 7.51 (m, 2H$_m$), 7.60 (m, 1H$_p$), 7.99 (m, 2H$_o$); ^{13}C NMR ($CDCl_3$): 23.30–24.85 (4C, NCHCH$_3$), 26.88/31.34 (2C, OCCH$_3$), 47.89–48.05 (4C, NCHCH$_3$), 53.65 (C_4), 66.37 ($C_{5'}$), 67.82 (d, C_5, $^1J_{CP} = 84.9$ Hz), 74.74 (d, $C_{4'}$, $^3J_{PC} = 13.8$ Hz), 109.08 ($C_{2'}$), 128.94 (2C_o), 129.39 (2C_m), 134.10 (C_p), 140.22 (C_{ipso}), 150.03 (C_3); HRMS (EI) *m*/*z* calcd. for $C_{25}H_{42}N_4O_4PS_2$ (M).

4.5. General procedure for cycloadditions of diazomethane to olefins (*Z*)-7 and (*E*)-7

A typical experiment is described for the synthesis of pyrazoline **16**. An ethereal solution of excess diazomethane was distilled onto a solution of (*E*)-**7** (130 mg, 0.5 mmol) in ether (22 mL). The light-protected resultant solution was stirred at rt overnight, then excess diazomethane was destroyed by addition of $CaCl_2$, and solvent was removed to afford **16** as a yellowish oil (124 mg, 98% yield). On standing as an ethereal solution at rt for 24 h, this compound was converted into the tautomer **17**, as a pasty solid unsuitable for microanalysis.

Attempts to purify oily pyrazolines **15** and **16** by chromatographic techniques resulted in Δ^1/Δ^2 isomerization and/or partial decomposition. Consequently, these compounds were only characterized by their NMR spectroscopic data as follows.

Compound 16: ^{1}H NMR ($CDCl_3$): 1.00 (s, 3H, *cis*-2′-CH_3), 1.05 (s, 3H, *trans*-2′-CH_3), 1.13 (s, 3H, O_2CCH_3), 1.5–2.4 (complex absorption, 5H, H_4, $H_{1'}$, $H_{3'}$, $2H_{4'}$), 3.70 (s, 3H, OCH_3), 3.70–4.03 (complex absorption, 5H, -OCH_2CH_2O-, H_5), 4.76 (dd, 1H, H_5, $^2J=17.0$, $^3J=8.6$), 5.29 (dd, 1H, H_3, $^3J=9.3$, $^3J'=2.3$); ^{13}C NMR (acetone-d_6): 18.11 (*cis*-2′-CH_3), 23.80 ($C_{4'}$), 24.35 (O_2CCH_3), 31.64 (*trans*-2′-CH_3,), 38.42 (C_4), 41.74 ($C_{2'}$), 49.69/52.26 ($C_{1'}$, $C_{3'}$), 53.73 (OCH_3), 64.09/65.85 (2C, -OCH_2CH_2O-), 80.67 (C_5), 89.55 (C_3), 110.09 (O_2CCH_3), 167.93 (*C*=O).

Compound 17: ^{1}H NMR ($CDCl_3$): 0.99 (s, 3H, *cis*-2′-CH_3); 1.11 (s, 3H, *trans*-2′-CH_3), 1.17 (s, 3H, O_2CCH_3), 1.36–1.54 (m, 2H, $H_{4'}$), 1.79–1.89 (m, 1H, $H_{3'}$), 1.97–2.05 (m, 1H, $H_{1'}$), 2.24–2.36 (m, 1H, $H_{3'}$), 3.75 (s, 3H, OCH_3), 3.74–3.95 (complex absorption, 4H, -OCH_2CH_2O-), 4.25 (ddd, 1H, H_{5a}, $^2J=17.91$, $^3J=4.48$, $^3J'=1.25$), 4.55 (ddd, 1H, H_{5b}, $^2J=17.91$, $^3J=8.42$, $^3J'=2.51$), 4.90 (m, 1H, H_3); ^{13}C NMR (acetone-d_6): 18.01 (*cis*-2′-CH_3), 23.90 ($C_{4'}$), 24.6 (O_2CCH_3), 31.83 (*trans*-2′-CH_3), 37.66 (C_4), 41.49 ($C_{2'}$), 46.56 ($C_{1'}$), 49.61 ($C_{3'}$), 52.72 (OCH_3), 64.11/65.90 (2C, -OCH_2CH_2O-), 82.08 (C_5), 93.63 (C_3), 109.99 (O_2CCH_3), 169.37 (*C*=O).

Compound 18: $[\alpha]_D$ −22.5 (*c* 2.00, CH_2Cl_2); IR (KBr) 3331, 1709; ^{1}H NMR ($CDCl_3$): 1.05 (s, 3H, *cis*-2′-CH_3), 1.15 (s, 3H, *trans*-2′-CH_3), 1.20 (s, 3H, O_2CCH_3), 1.67 (m, 1H, $H_{4'a}$), 1.85 (m, 1H, $H_{4'b}$), 2.04 (complex absorption, 2H, $H_{1'}$, $H_{3'}$), 3.30 (m, 1H, H_4), 3.55 (m, 2H, H_{5a}, H_{5b}), 3.80 (s, 3H, OCH_3), 3.78–4.00 (complex absorption, 4H, -OCH_2CH_2O-); ^{13}C NMR ($CDCl_3$): 16.85 (*cis*-2′-CH_3), 22.61 ($C_{4'}$), 23.68 (O_2CCH_3), 30.75 (*trans*-2′-CH_3), 42.14 ($C_{2'}$), 42.37 (C_4), 43.24 ($C_{1'}$), 49.10 ($C_{3'}$), 51.90 (OCH_3), 53.27 (C_5), 63.60/65.45 (2C, -OCH_2CH_2O-), 109.85(O_2CCH_3), 146.37 (C_3), 163.06 (*C*=O).

Acknowledgements

The authors thank Dr. T. Parella, NMR Service at the UAB, for his assistance in the performance and interpretation of NOE experiments. Thanks are due to the Bilateral Cooperation Program (Acción Integrada HF99-0083, Spain, and Picasso 00637QA, France). Financial supports of the CNRS (France) and through the project PB97-0214 (Spain) are gratefully acknowledged. Access to the facilities of the Catalonia Supercomputer Center (CESCA) is gratefully acknowledged.

References

1. For some recent articles and reviews, see: (a) Burgess, K.; Moye-Sherman, D.; Ho K.-K. *Synlett* **1994**, 575; (b) Jiménez, J. M.; Rifé, J.; Ortuño, R. M. *Tetrahedron: Asymmetry* **1996**, *7*, 537; (c) Jiménez, J. M.; Ortuño, R. M. *Tetrahedron: Asymmetry* **1996**, *7*, 3203; (d) Rifé, J.; Ortuño, R. M.; Lajoie, G. A. *J. Org. Chem.* **1999**, *64*, 8958; (e) Illescas, B.; Rifé, J.; Ortuño, R. M.; Martin, N. *J. Org. Chem.* **2000**, *65*, 6246; (f) Cativiela, C.; Diaz-De-Villegas, M. D. *Tetrahedron: Asymmetry* **2000**, *11*, 645; (g) Füllöp, F. *Chem. Rev.* **2001**, *101*, 2181 and references cited therein.
2. (a) Burgess, K.; Li, W.; Lim, D.; Moye-Sherman, D. *Biopolymers* **1997**, *42*, 439; (b) Díaz, M.; Jiménez, J. M.; Ortuño, R. M. *Tetrahedron: Asymmetry* **1997**, *8*, 2465; (c) Martin, S. F.; Dorsey, G. O.; Gane, T.; Hillier, M. C.; Kessler, H.; Baur, M.; Mathae, B.; Erickson, J. W.; Bhat, T. N.; Munshi, S.; Gulnik, S. V.; Topol, I. A. *J. Med. Chem.* **1998**, *41*, 1581; (d) Moye-Sherman, D.; Jin, S.; Li, S.; Welch, M. B.; Reibenspies, J.; Burgess, K. *Chem.-Eur. J.* **1999**, *5*, 2730; (e) Martin, S. F.; Dwyer, M. P.; Hartmann, B.; Knight, K. S. *J. Org. Chem.* **2000**, *65*, 1305; (f) Davidson, J. P.; Martin, S. F. *Tetrahedron Lett.* **2000**, *41*, 9459; (g) Hillier, M. C.; Davidson, J. P.; Martin, S. F. *J. Org. Chem.* **2001**, *66*, 1657.
3. (a) Harnden, M. R.; Jarvest, R. L.; Bacon, T. H.; Boyd, M. R. *J. Med. Chem.* **1987**, *30*, 1636; (b) Yang, T.-F.; Kim, H.; Kotra, L. P.; Chu, C. K. *Tetrahedron Lett.* **1996**, *49*, 8849; (c) Csuk, R.; von Scholz, Y. *Tetrahedron* **1994**, *50*, 10431; (d) Csuk, Y.; von Scholz, Y. *Tetrahedron* **1995**, *51*, 7193; (e) Zhao, Y.; Yang, T.; Lee, D.; Newton, M. G.; Chu, C. K. *J. Org. Chem.* **1995**, *60*, 5236; (f) Lee, G.; Du, J. F.; Chun, M. W.; Chu, C. K. *J. Org. Chem.* **1997**, *62*, 1991; (g) Csuk, R.; Eversmann, L. *Tetrahedron* **1998**, *54*, 6445; (h) Csuk, R.; Thiede, G. *Tetrahedron* **1999**, *55*, 739; (i) Csuk, R.; Kern, A. *Tetrahedron* **1999**, *55*, 8409; (j) Gauvry, N.; Huet, F. *Tetrahedron* **1999**, *55*, 1321; (k) Rifé, J.; Ortuño, R. M. *Org. Lett.* **1999**, *1*, 1221; (l) Chen, X.; Zemlika, J. *J. Org. Chem.* **2002**, *67*, 286.
4. (a) Chan, D. M. T.; Stevenson, T. M.; Piotrowski, D. W.; Fahmy, M. A. H.; Lowe, R. L.; Monaco, K. L.; Reeves, B. M.; Folgar, M. P.; Esrey, E. G. *Book of Abstracts, 217th ACS National Meeting, Anaheim, CA, March 21–25 (1999), AGRO-029*. AN 1999:91067; (b) Fathalla, O. A.; Gad, H. S. M.; Maghaby, A. S. *Arch. Pharmacol. Res.* **2000**, *23*, 128. CAN 133:212964; (c) Bharmal, F. M.; Kaneriya, D. J.; Parekh, H. H. *Indian J. Heterocyclic Chem.* **2001**, *10*, 189. CAN 2001:323266.
5. Jiménez, J. M.; Bourdelande, J. L.; Ortuño, R. M. *Tetrahedron* **1997**, *53*, 3777.
6. (a) Houk, K. N.; Moses, S. R.; Wu, Y.-D.; Rondan, N. G.; Jäger, V.; Schohe, R.; Fronczek, F. R. *J. Am. Chem. Soc.* **1984**, *106*, 3880; (b) Houk, K. N.; Duh, H.-Y.; Moses, S. R. *J. Am. Chem. Soc.* **1986**, *108*, 2754; (c) Raimondi, L.; Wu, Y.-D.; Brown, F. K.; Houk, K. N. *Tetrahedron Lett.* **1992**, *33*, 4409.
7. (a) Hoffmann, R. W. *Chem. Rev.* **1989**, *89*, 1841; (b) Broeker, J. L.; Hoffmann, R. W.; Houk, K. N. *J. Am. Chem. Soc.* **1991**, *113*, 5006.
8. See, for instance: (a) Reetz, M. T.; Kayser, F.; Harms, K. *Tetrahedron Lett.* **1992**, *33*, 3453; (b) Galley, G.; Pätzel, M.; Jones, P. G. *Tetrahedron* **1995**, *51*, 1631; (c) Annunziata, R.; Benaglia, M.; Cinquini, M.; Cozzi, F.; Raimondi, L. *Electronic Conference on Heterocyclic Chemistry (ECHET96)*. CD-ROM included in *J. Chem. Soc., Chem. Commun.* **1997**, no. 6; (d) Martín-Vilà, M.; Hanafi, N.; Jiménez, J. M.; Álvarez-Larena, A.; Piniella, J. F.; Branchadell, V.; Oliva, A.; Ortuño, R. M. *J. Org. Chem.* **1998**, *63*, 3581.
9. Muray, E.; Álvarez-Larena, A.; Piniella, J. F.; Branchadell, V.; Ortuño, R. M. *J. Org. Chem.* **2000**, *65*, 388.
10. Moglioni, A.; García-Expósito, E.; Álvarez-Larena, A.; Branchadell, V.; Moltrasio, G. Y.; Ortuño, R. M. *Tetrahedron: Asymmetry* **2000**, *11*, 4903.

11. Baceiredo, A.; Bertrand, G.; Sicard, G. *J. Am. Chem. Soc.* **1985**, *107*, 4781.
12. Goumri-Magnet, S.; Kato, T.; Gornitzaka, H.; Baceiredo, A.; Bertrand, G. *J. Am. Chem. Soc.* **2000**, *122*, 4464.
13. Mann, J.; Partlett, N. K.; Thomas, A. *J. Chem. Res. (S)* **1987**, 369.
14. (a) For the synthesis of (*Z*)-**2**, see: Shahhak, I.; Almog, J. *Synthesis* **1970**, 145; (b) For (*E*)-**2**, see: Craig, D.; Ley, S. V.; Simptkins, N. S. *J. Chem. Soc., Perkin Trans. 1* **1985**, 1949.
15. Ibuka, T.; Akimoto, N.; Tanaka, M.; Nishii, S.; Yamamoto, Y. *J. Org. Chem.* **1989**, *54*, 4055.
16. Galley, G.; Hübner, J.; Anklam, S.; Jones, P. G.; Pätzel, M. *Tetrahedron Lett.* **1996**, *37*, 6307.
17. Moglioni, A. G.; Muray, E.; Castillo, J. A.; Álvarez-Larena, A.; Moltrasio, G.; Branchadell, V.; Ortuño, R. M. *J. Org. Chem.* **2002**, *66*, 2402.
18. The configuration of the new stereogenic centre was established by considering the stereochemistry relative to the centre derived from D-glyceraldehyde.
19. Becke, A. D. *Phys. Rev. A* **1988**, *38*, 3098.
20. (a) Wang, Y.; Perdew, J. P. *Phys. Rev. B* **1991**, *44*, 13298; (b) Perdew, J. P.; Chevary, J. A.; Vosko, S. H.; Jackson, K. A.; Pederson, M. R.; Singh, D. J.; Fiolhais, C. *Phys. Rev. B* **1992**, *46*, 6671.
21. Branchadell, V.; Muray, E.; Oliva, A.; Ortuño, R. M.; Rodríguez-García, C. *J. Phys. Chem. A* **1998**, *102*, 10106.
22. Hehre, W. J.; Radom, L.; Schleyer, P.v. R.; Pople, J. A. *Ab Initio Molecular Orbital Theory*; Wiley: New York, 1986.
23. Gaussian 98, Revision A.6, Frisch, M. J.; Trucks, G. W.; Schlegel, H. B.; Scuseria, G. E.; Robb, M. A.; Cheeseman, J. R.; Zakrzewski, V. G.; Montgomery, Jr., J. A.; Stratmann, R. E.; Burant, J. C.; Dapprich, S.; Millam, J. M.; Daniels, A. D.; Kudin, K. N.; Strain, M. C.; Farkas, O.; Tomasi, J.; Barone, V.; Cossi, M.; Cammi, R.; Mennucci, B.; Pomelli, C.; Adamo, C.; Clifford, S.; Ochterski, J.; Petersson, G. A.; Ayala, P. Y.; Cui, Q.; Morokuma, K.; Malick, D. K.; Rabuck, A. D.; Raghavachari, K.; Foresman, J. B.; Cioslowski, J.; Ortiz, J. V.; Stefanov, B. B.; Liu, G.; Liashenko, A.; Piskorz, P.; Komaromi, I.; Gomperts, R.; Martin, R. L.; Fox, D. J.; Keith, T.; Al-Laham, M. A.; Peng, C. Y.; Nanayakkara, A.; Gonzalez, C.; Challacombe, M.; Gill, P. M. W.; Johnson, B.; Chen, W.; Wong, M. W.; Andres, J. L.; Gonzalez, C.; Head-Gordon, M.; Replogle, E. S.; Pople, J. A. Gaussian, Inc., Pittsburgh PA, 1998. http://www.gaussian.com.
24. (a) ADF 1999, Baerends, E. J.; Bérces, A.; Bo, C.; Boerrigter, P. M.; Cavallo, L.; Deng, L.; Dickson, R. M.; Ellis, D. E.; Fan, L.; Fischer, T. H.; Fonseca Guerra, C.; van Gisbergen, S. J. A.; Groeneveld, J. A.; Gritsenko, O. V.; Harris, F. E.; van den Hoek, P.; Jacobsen, H.; van Kessel, G.; Kootstra, F.; van Lenthe, E.; Osinga, V. P.; Philipsen, P. T. H.; Post, D.; Pye, C. C.; Ravenek, W.; Ros, P.; Schipper, P. R. T.; Schreckenbach, G.; Snijders, J. G.; Solà, M.; Swerhone, D.; te Velde, G.; Vernooijs, P.; Versluis, L.; Visser, O.; van Wezenbeek, E.; Wiesenekker, G.; Wolff, S. K.; Woo, T. K.; Ziegler, T. Scientific Computing & Modelling NV, Amsterdam, The Netherlands, 1999. http://www.scm.com; (b) Fonseca Guerra, C.; Snijders, J. G.; te Velde, G.; Baerends, E. J. *Theor. Chem. Acc.* **1998**, *99*, 391.
25. Sheldrick, G. M. *Acta Crystallogr.* **1997**, *A46*, 467–473.
26. SHELXL-97, Program for Crystal Structure Refinement, Sheldrick, G. M., University of Göttingen, 1997.